

## Inventory of supplemental information

<b>Supplemental Figures</b>	<b>Related to main figure</b>
Figure S1. Rubicon interactions with p22 <i>phox</i> -gp91 <i>phox</i> complex.	Figure 1
Figure S2. Rubicon interactions with Beclin-1-UVRAG complex and p22 <i>phox</i> -gp91 <i>phox</i> complex.	Figure 2
Figure S3. Rubicon affects p22 <i>phox</i> localization.	Figure 3
Figure S4. Rubicon enhances phagocytosis in a p22 <i>phox</i> -binding-dependent manner.	Figure 4
Figure S5. Rubicon enhances TLR signal transduction.	Figure 5
Figure S6. <i>In vivo</i> Rubicon expression in infected mice.	Figure 6
Figure S7. Rubicon plays distinctive roles in conventional and TLR signaling-mediated autophagy.	Figure 7

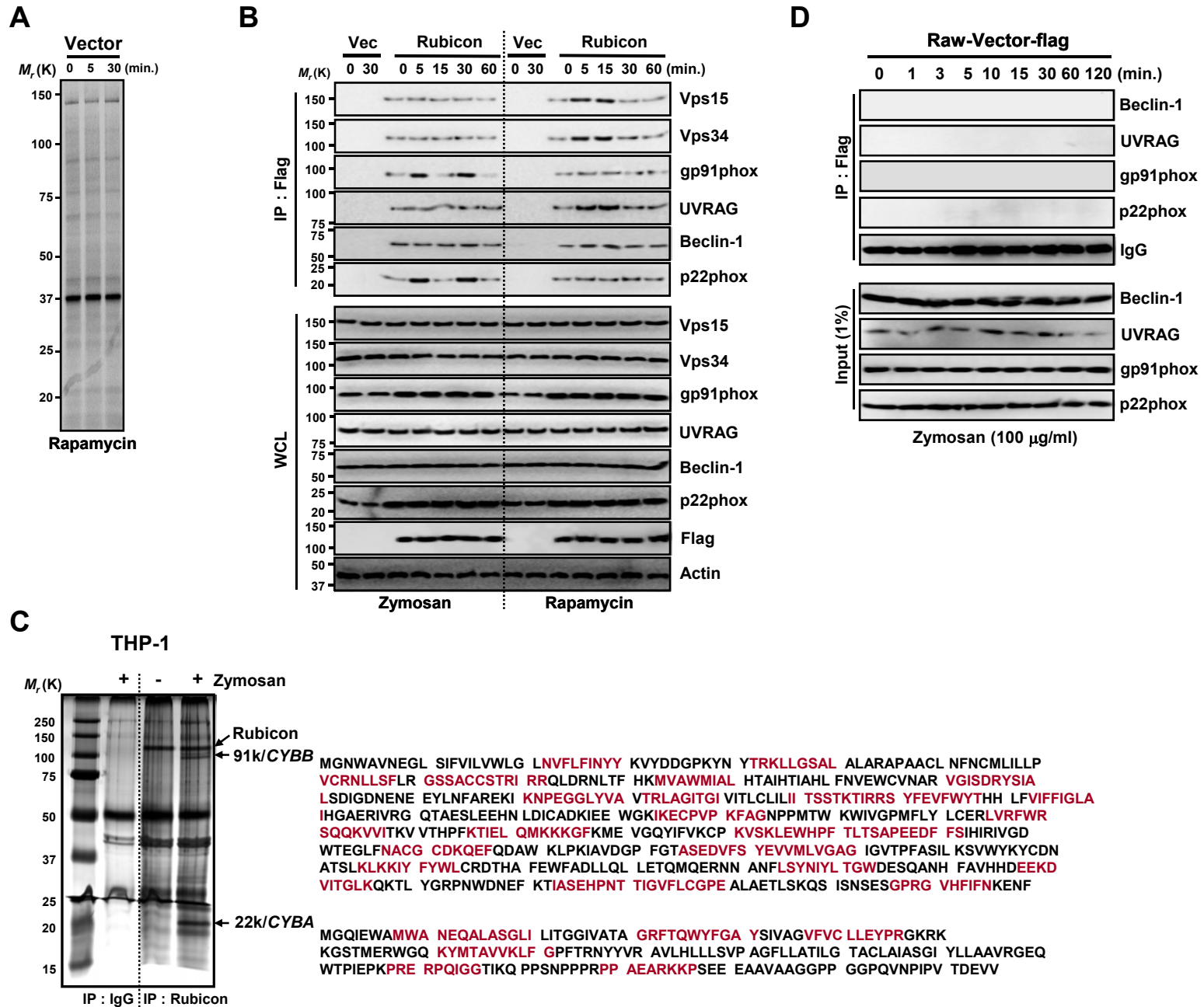
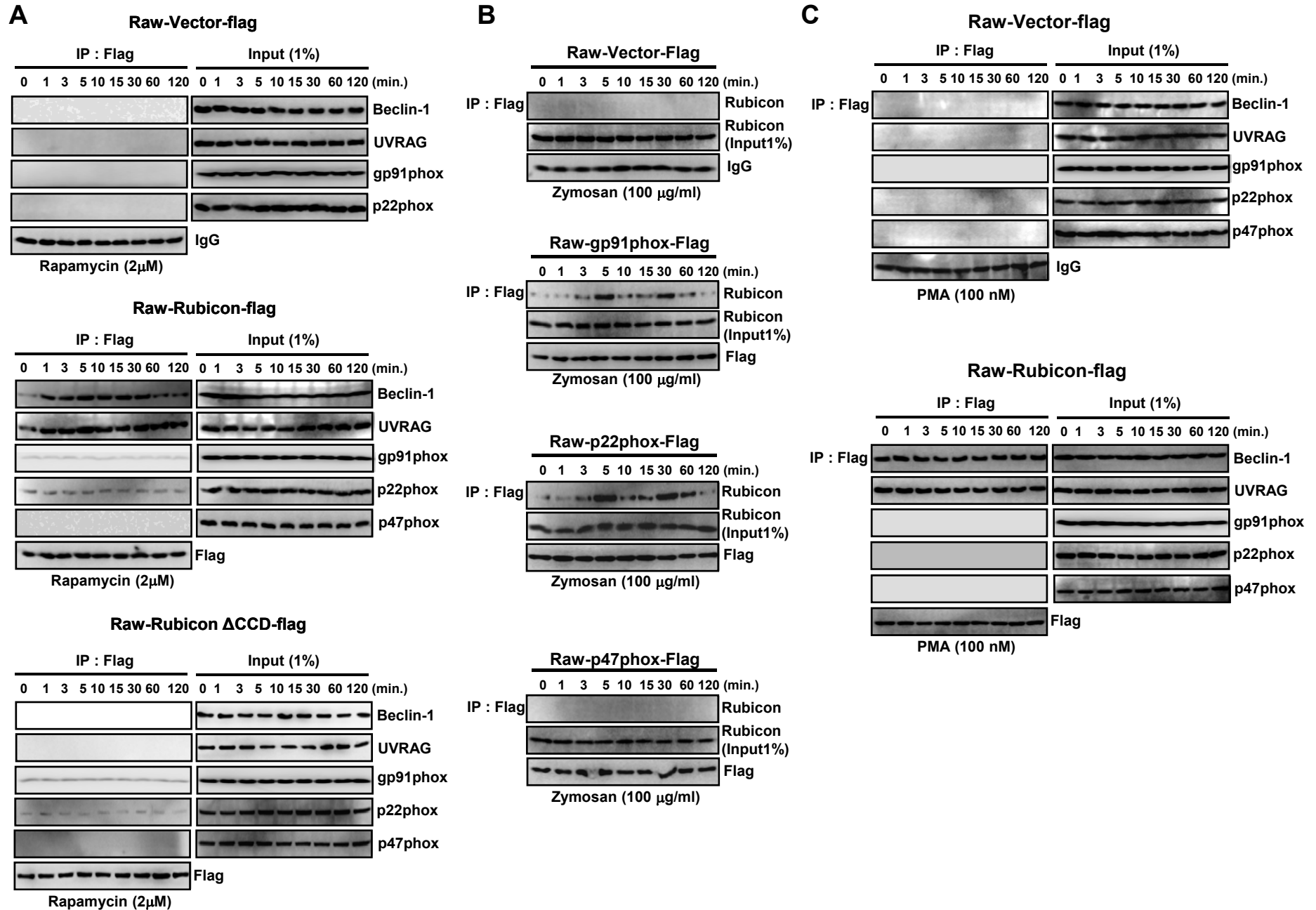
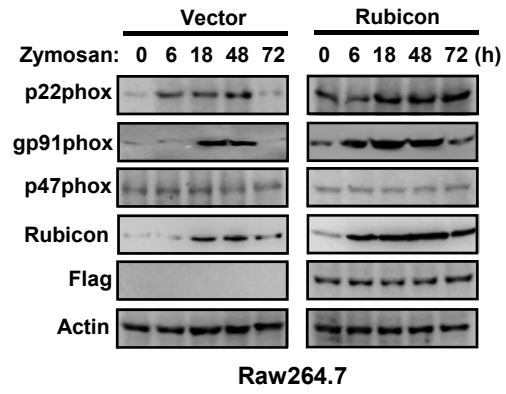
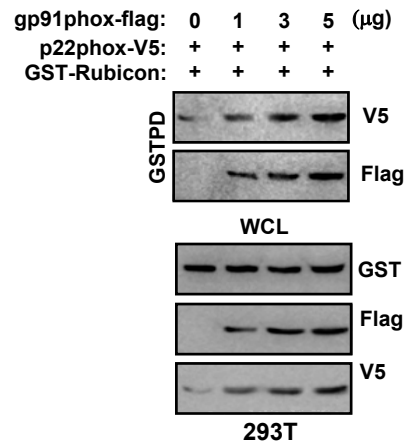
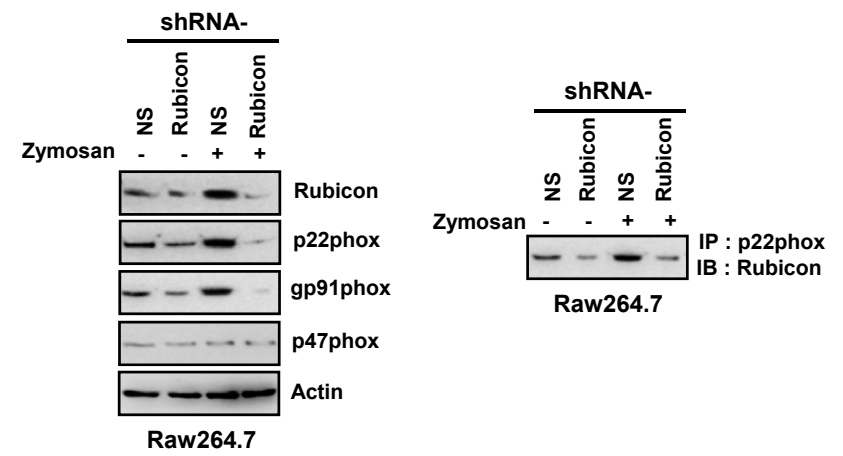


Fig S1



**Fig S2**

**D****E****F****Fig S2**

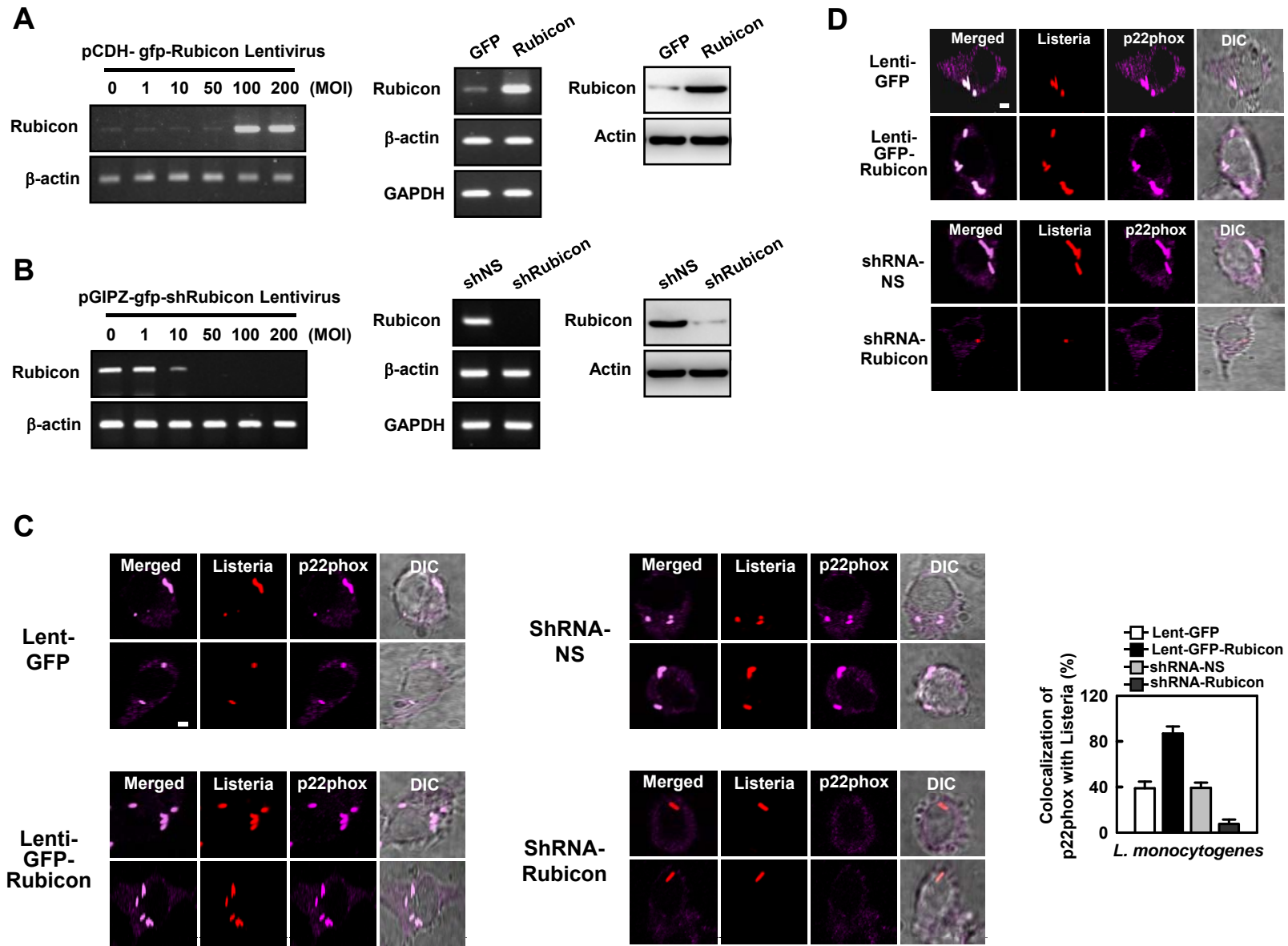
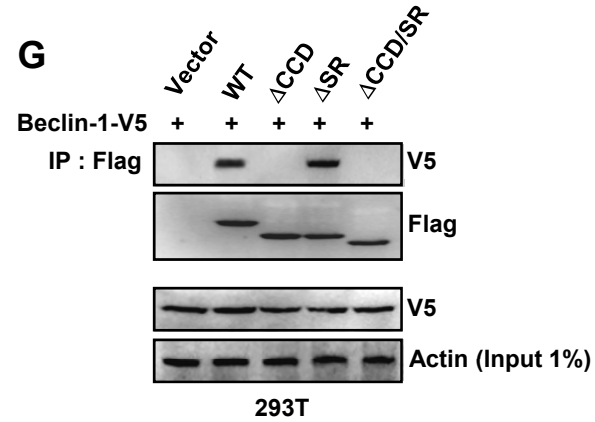
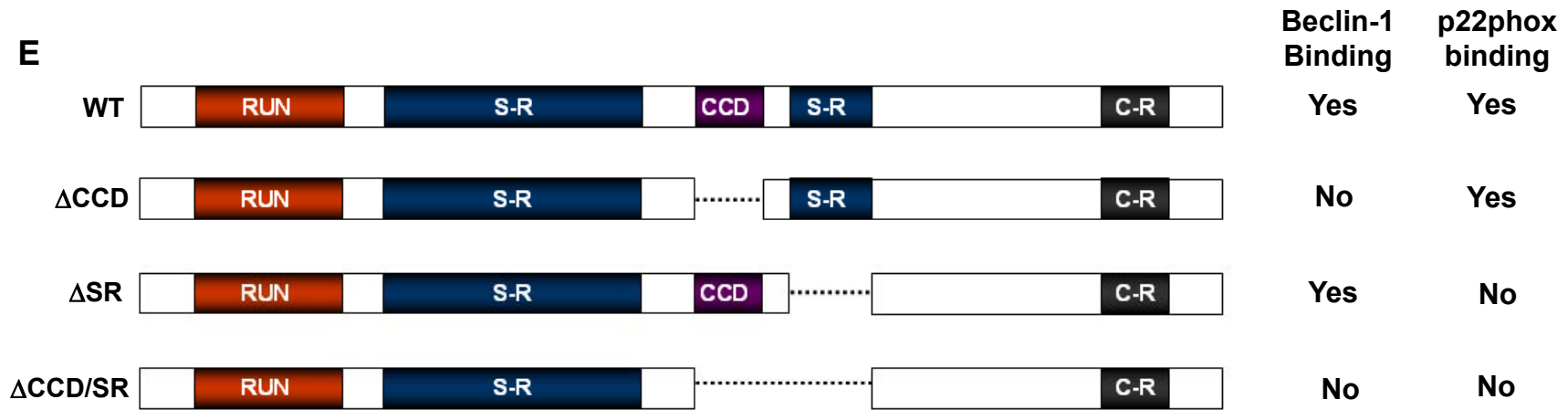
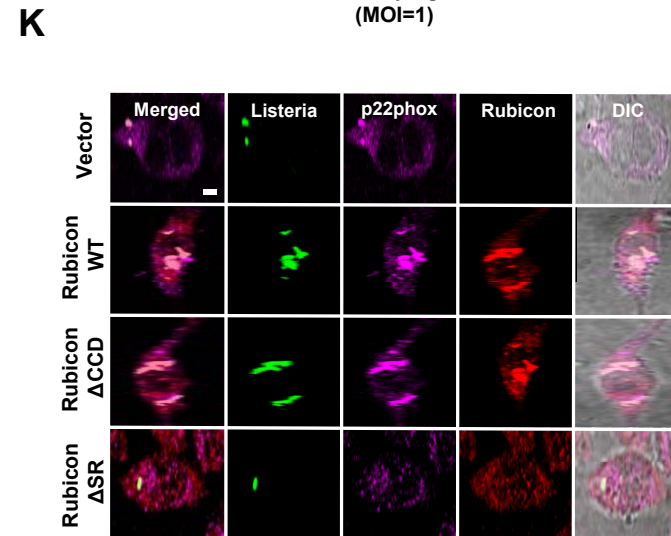
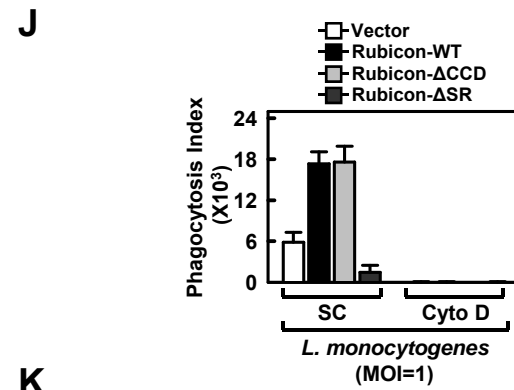
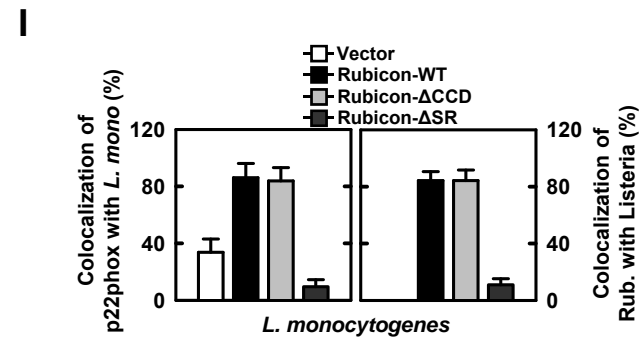
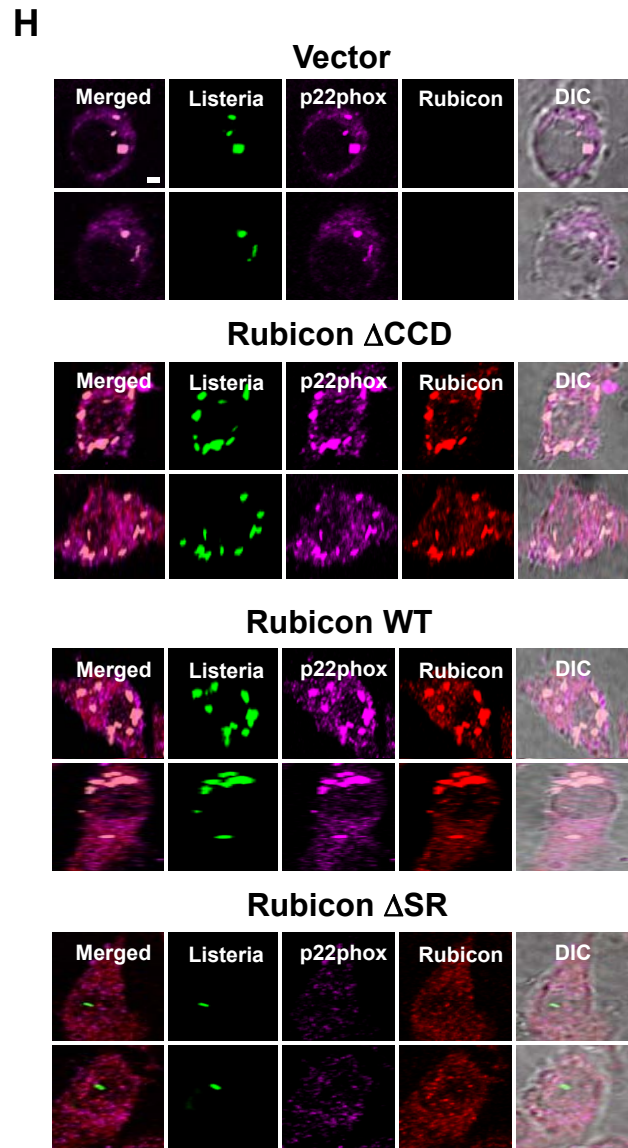


Fig S3



**Fig S3**



**Fig S3**

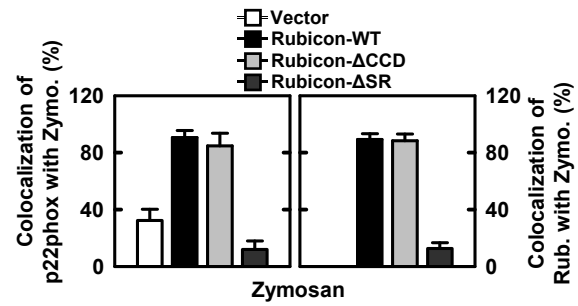
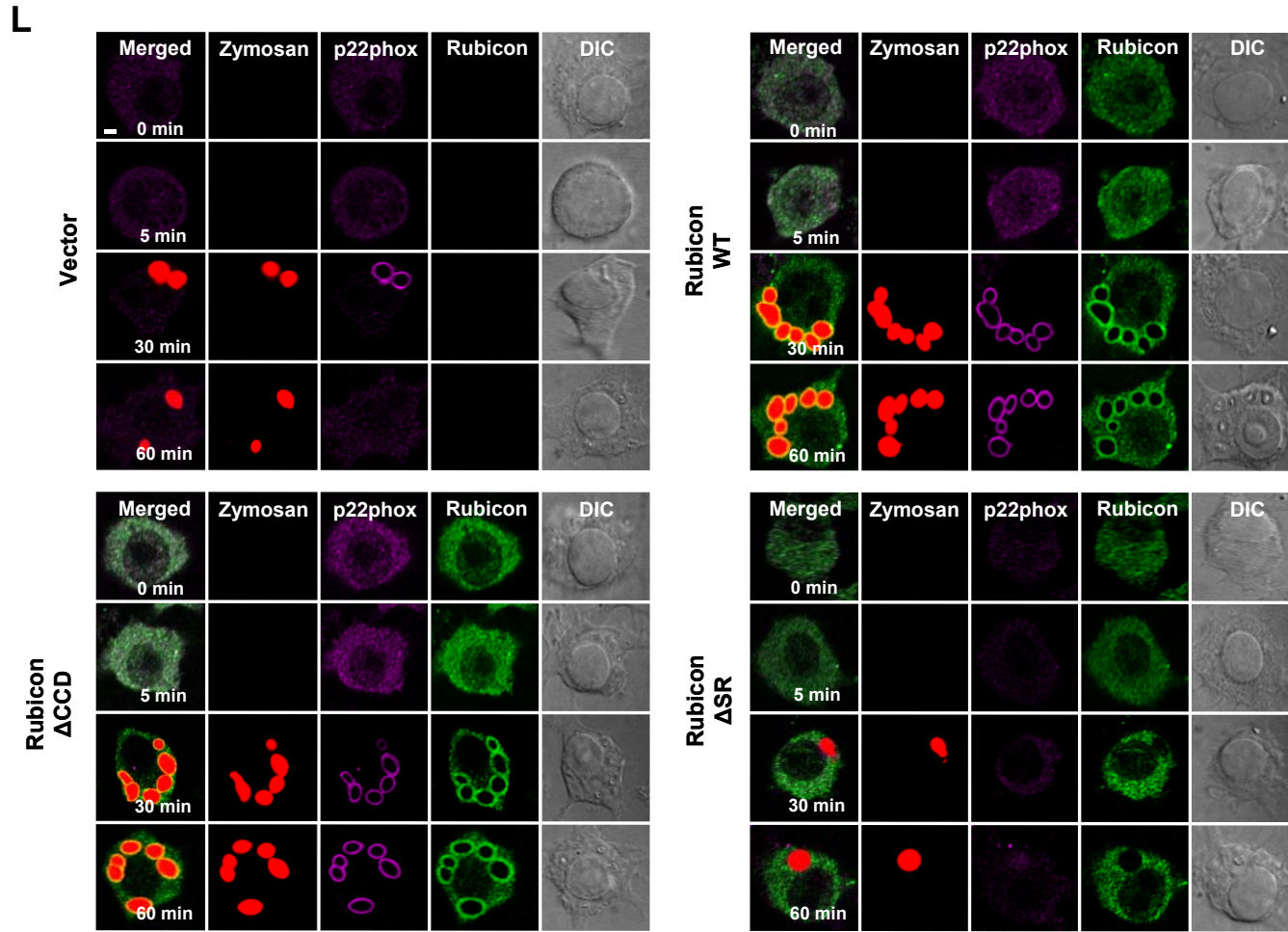


**Fig S3**



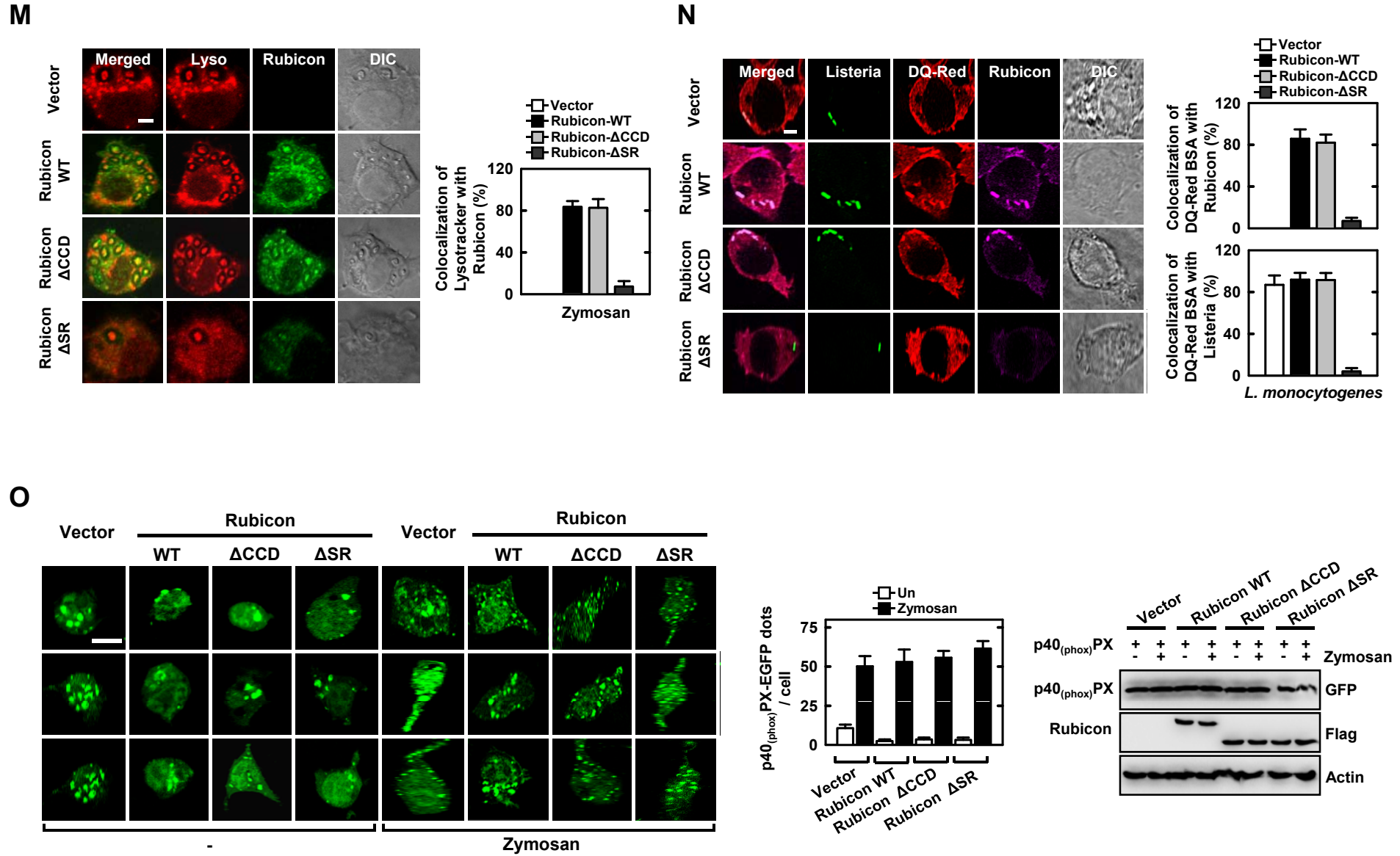


**Fig S3**

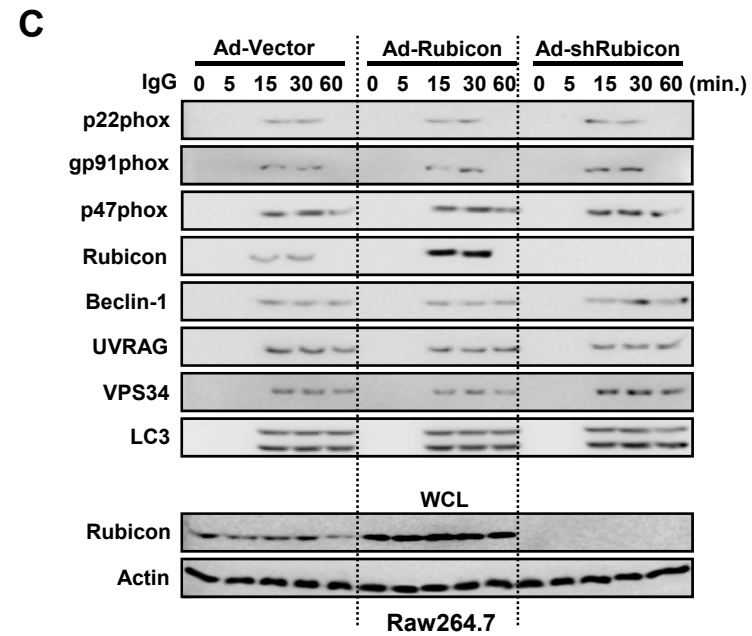
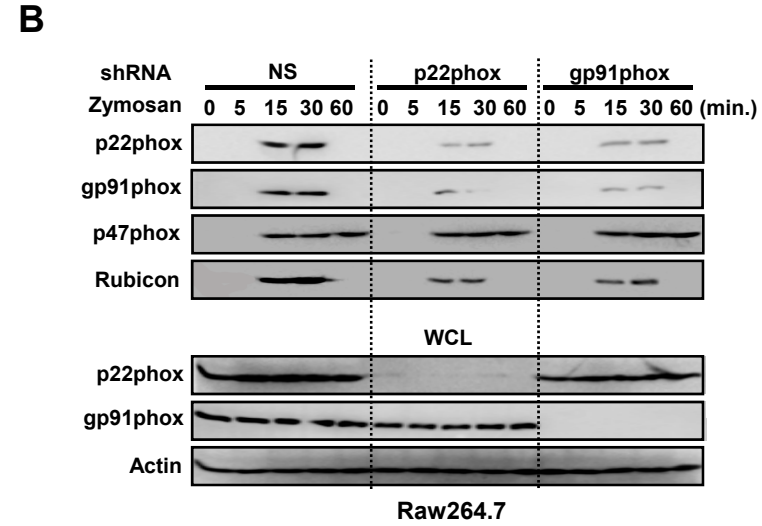
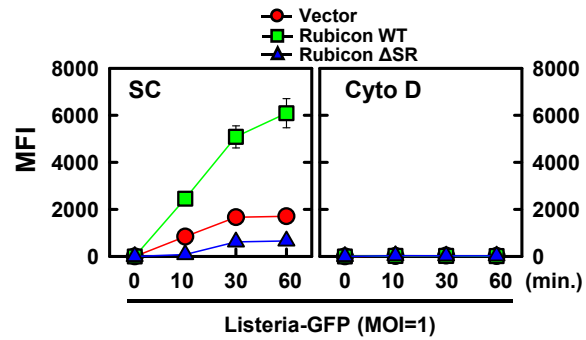
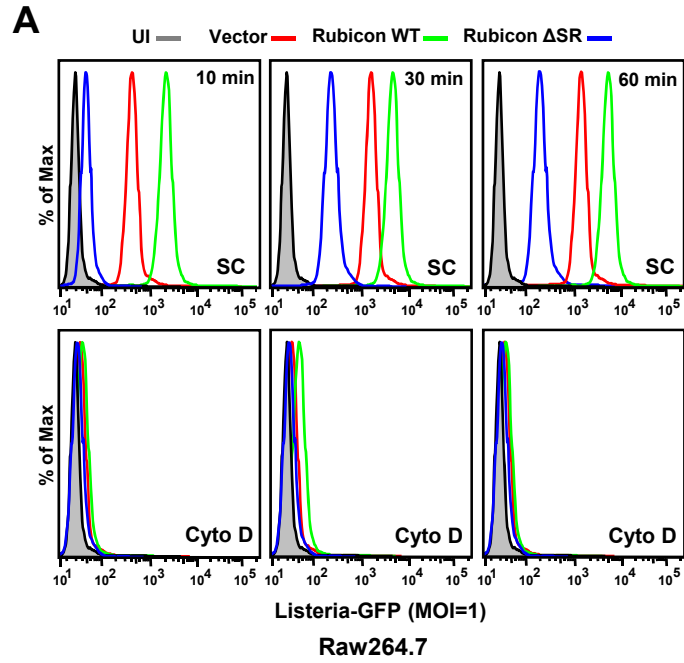
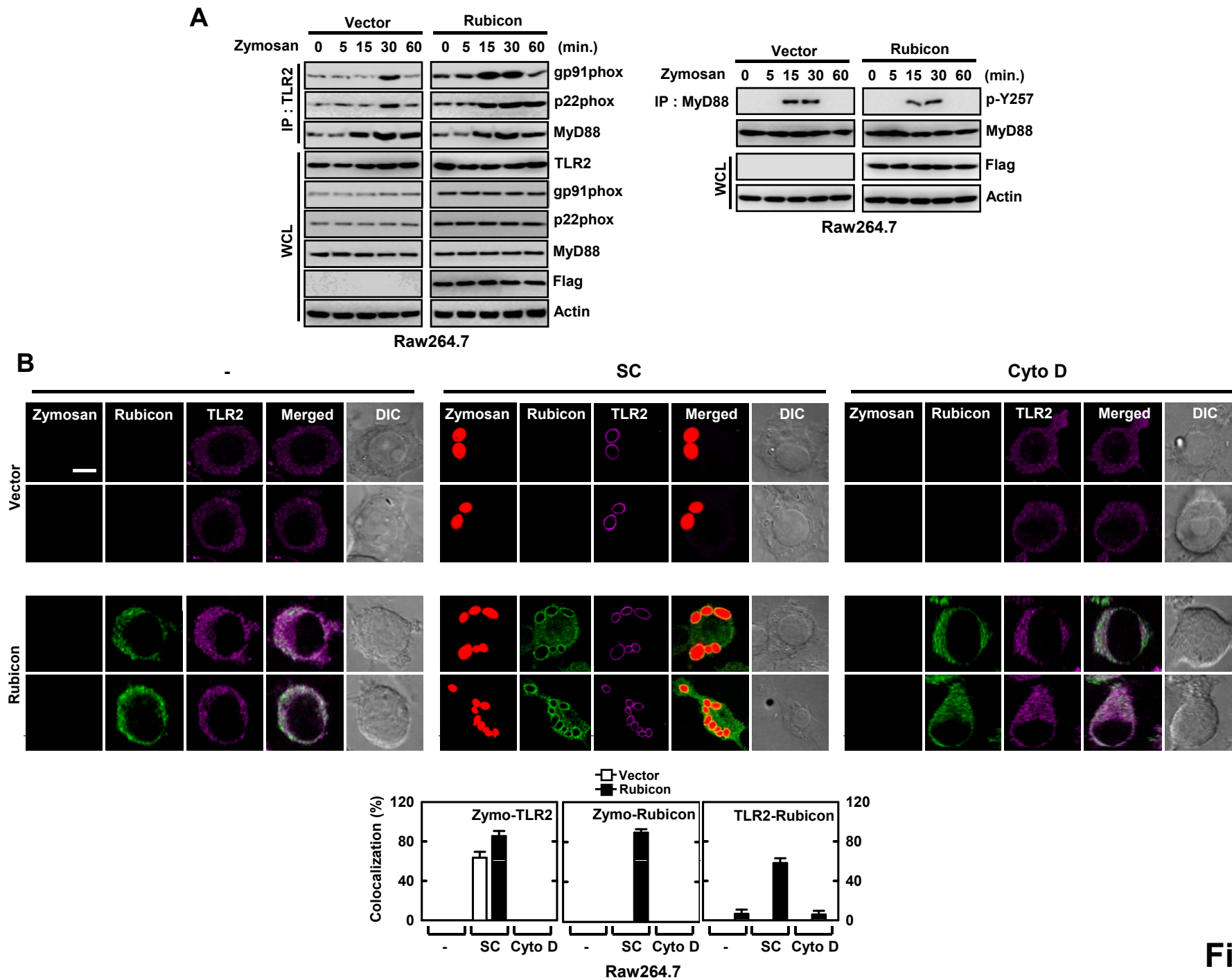


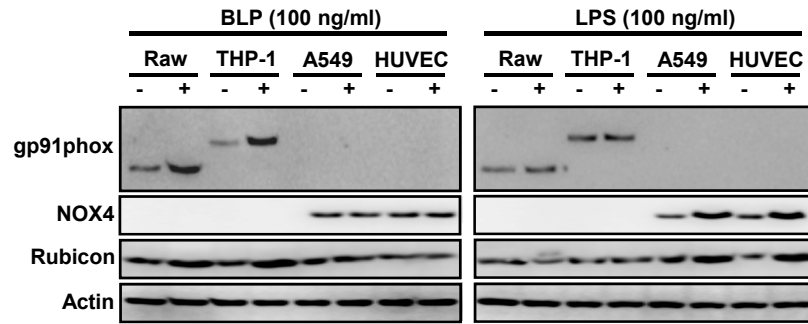
Fig S4



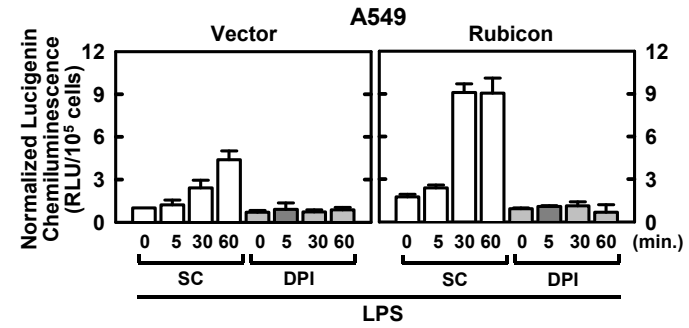


**Fig S5**

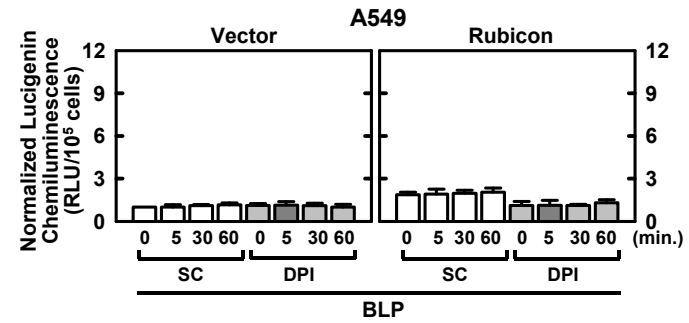
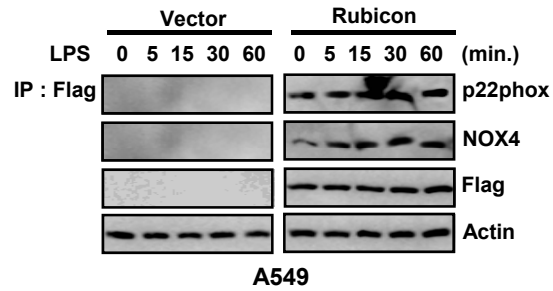
**C**



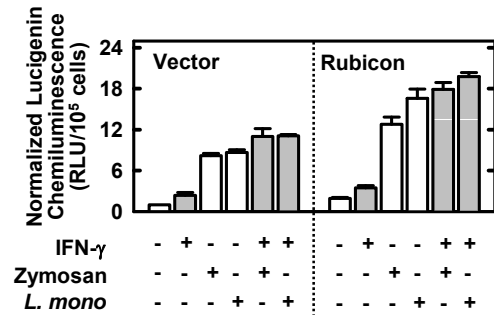
**E**



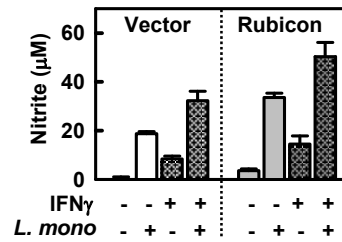
**D**



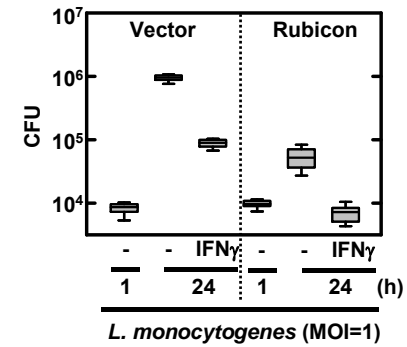
**F**



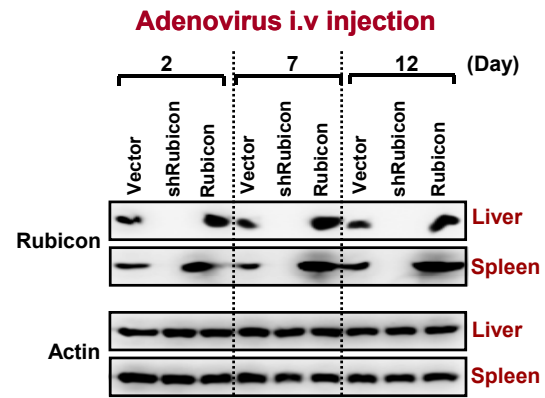
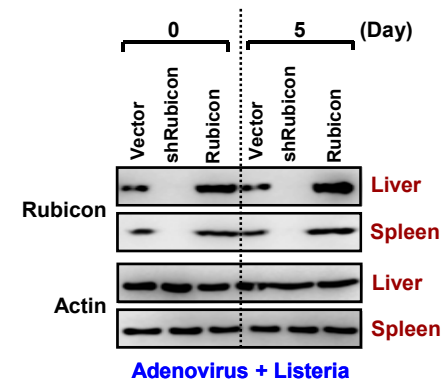
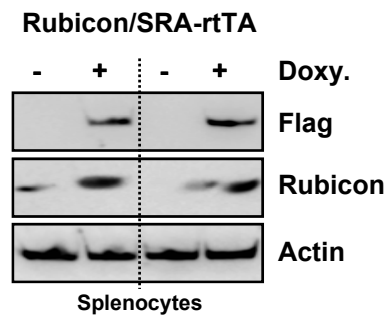
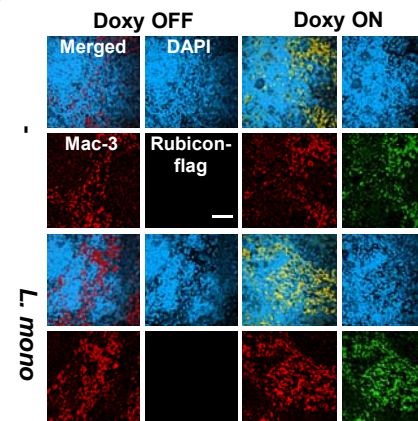
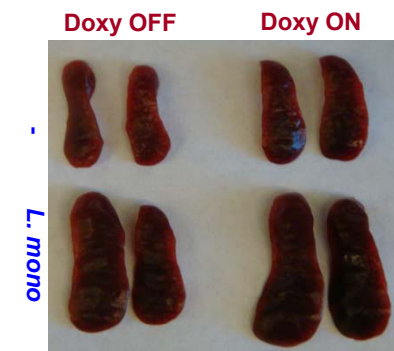
**G**

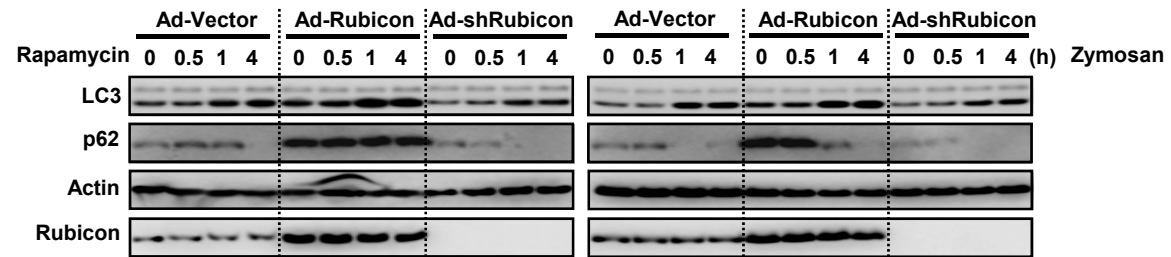
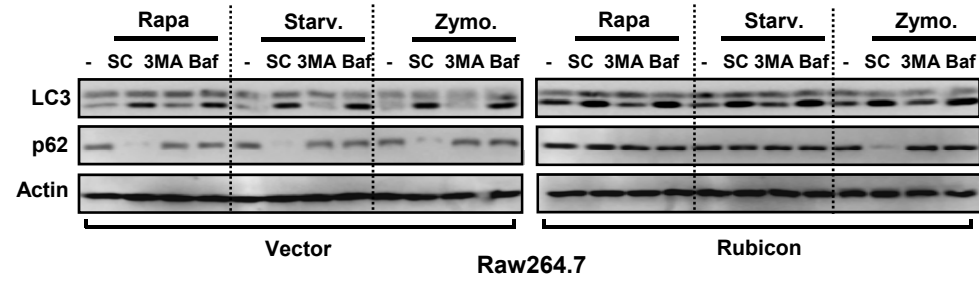


**H**



**Fig S5**

**A****B****C****D****E****Fig S6**

**A****B****Fig S7**

# Supplemental Information

## Supplementary Figure Legends

### Figure S1. Rubicon interactions with p22*phox*-gp91*phox* complex.

**(A)** Radio-actively labeled THP-1 cells containing vector were stimulated with rapamycin (2 $\mu$ M) for the indicated times, followed by IP with  $\alpha$ Flag for autoradiography. **(B)** Differential Rubicon interactions. Raw264.7 cells containing vector or Flag-Rubicon WT were stimulated with 100 $\mu$ g/ml zymosan or 2 $\mu$ M rapamycin for indicated times, followed by IP with  $\alpha$ Flag and IB with  $\alpha$ Vps15,  $\alpha$ Vps34,  $\alpha$ gp91*phox*,  $\alpha$ UVRAG,  $\alpha$ Beclin-1,  $\alpha$ p22*phox*,  $\alpha$ Actin or  $\alpha$ Flag. **(C)** Identification of p22*phox* (CYBA) and gp91*phox* (CYBB) as Rubicon-binding proteins. Rubicon complexes purified from THP-1 cells with or without zymosan stimulation were subjected to Mass Spectrometry analysis. The red-colored letters indicate the peptides identified from mass spectrometry analysis. **(D)** Raw264.7 cells containing vector were stimulated with zymosan for indicated times, followed by IP with  $\alpha$ Flag and IB with  $\alpha$ Beclin-1,  $\alpha$ UVRAG,  $\alpha$ gp91*phox*,  $\alpha$ p22*phox* or  $\alpha$ Flag.

### Figure S2. Rubicon interactions with Beclin-1-UVRAG complex and p22*phox*-gp91*phox* complex.

**(A)** Rubicon interaction with Beclin-1-UVRAG complex. Raw264.7 cells containing vector, Flag-Rubicon WT or  $\Delta$ CCD were stimulated with 2 $\mu$ M rapamycin for indicated times (min), followed by IP with  $\alpha$ Flag and IB with  $\alpha$ Beclin-1,  $\alpha$ UVRAG,  $\alpha$ gp91*phox*,  $\alpha$ p22*phox*,  $\alpha$ p47*phox*, or  $\alpha$ Flag. **(B)** Rubicon interaction with p22*phox* and gp91*phox* complex. Raw264.7 cells containing vector, Flag-gp91*phox*, Flag-p22*phox* or Flag-p47*phox* were stimulated with 100 $\mu$ g/ml zymosan for indicated times, followed by IP with  $\alpha$ Flag and IB with  $\alpha$ Rubicon or  $\alpha$ Flag. **(C)** PMA stimulation



does not induce Rubicon interaction with p22*phox* and gp91*phox* complex. Raw264.7 cells containing vector or Flag-Rubicon WT were stimulated with 100nM PMA for indicated times, followed by IP with  $\alpha$ Flag and IB with  $\alpha$ Beclin-1,  $\alpha$ UVRAG,  $\alpha$ gp91*phox*,  $\alpha$ p22*phox*,  $\alpha$ p47*phox*, or  $\alpha$ Flag. **(D)** Raw264.7 cells containing vector or Flag-Rubicon were stimulated with 100 $\mu$ g/ml zymosan for indicated times, followed by IB with  $\alpha$ gp91*phox*,  $\alpha$ p22*phox*,  $\alpha$ p47*phox*,  $\alpha$ Rubicon,  $\alpha$ Flag or  $\alpha$ Actin. **(E)** At 48h posttransfection with GST-Rubicon and V5-p22*phox* vector with increasing amount of Flag-gp91*phox* vector, 293T cell lysates were used for GST-PD, followed by IB with  $\alpha$ V5 or  $\alpha$ Flag. WCLs were used for IB with  $\alpha$ GST,  $\alpha$ Flag, or  $\alpha$ V5. **(F)** Depletion of Rubicon expression affects the levels of p22*phox* and gp91*phox* expression. At 48h postinfection with shRNA knockdown vector (lenti-shRNA-NS or lenti-shRNA-Rubicon, MOI=50), Raw246.7 cells were stimulated with or without zymosan for 18h and WCLs were used for IB with indicated antibodies (left) or IP with  $\alpha$ p22*phox* and IB with  $\alpha$ Rubicon (right).

**Figure S3. Rubicon affects p22*phox* localization.**

**(A, B, C and D)** Rubicon affects the p22*phox* localization. At 48 h postinfection with lenti-GFP-Rubicon **(A)** or lenti-shRNA-Rubicon **(B)** at various MOIs, Raw264.7 cells were used for RT-PCR for Rubicon and  $\beta$ -actin. At 48h postinfection with lenti-GFP or lenti-GFP-Rubicon at MOI=100 **(A)** or lenti-shRNA-NS or lenti-shRNA-Rubicon at MOI=50 **(B)**, Raw264.7 cells were used for RT-PCR for Rubicon,  $\beta$ -actin or GAPDH or IB with  $\alpha$ Rubicon or  $\alpha$ Actin. Raw264.7 cells were then infected with **(C)** heat-killed (HK)-TRITC-labeled *L. monocytogenes* (MOI=1) or **(D)** live-TRITC-labeled *L. monocytogenes* (MOI=1) for 30 min, followed by confocal microscopy with  $\alpha$ p22*phox*. Bar, 2  $\mu$ m. The right panel shows the colocalization index (%) between p22*phox* and GFP-*L. monocytogenes* determined by computer program.

**(E, F, and G)** Rubicon interactions with Beclin-1 and p22phox. **(E)** Schematic diagram of Rubicon structure and summary of Rubicon interactions with Beclin-1 and p22phox. **(F)** Flag-Rubicon WT and mutant expression in Raw264.7 cells. WCLs were used for IP with  $\alpha$ Flag and IB with  $\alpha$ Flag. **(G)** Beclin-1 interaction with Rubicon WT and mutants. At 48h posttransfection with indicated constructs, 293T cells lysates were used for IP with Flag, followed by IB with Flag or V5. WCLs were used for IB to show V5-Beclin-1 and Actin.

**(H, I, J, K and L)** Rubicon enhances the co-localization of p22phox with *L. monocytogenes*-containing phagosomes. **(H)** Raw264.7 cells containing vector, Flag-Rubicon WT,  $\Delta$ CCD or  $\Delta$ SR were infected with HK-GFP-*L. monocytogenes* (MOI=1) for 30 min, followed by confocal microscopy with  $\alpha$ p22phox and  $\alpha$ Flag. Bar, 2  $\mu$ m. **(I)** Colocalization index (%) between p22phox and GFP-*L. monocytogenes*. **(J)** Phagocytosis index (%) of GFP-*L. monocytogenes*. Treatment with the Cytochalasin D (Cyto D, 10 $\mu$ M), phagocytosis inhibitor, was included as a negative control. SC, solvent control. **(K)** Raw264.7 cells containing vector, Flag-Rubicon WT,  $\Delta$ CCD or  $\Delta$ SR were infected with Live-GFP-*L. monocytogenes* (MOI=1) for 30 min, followed by confocal microscopy with  $\alpha$ p22phox and  $\alpha$ Flag. Bar, 2  $\mu$ m. **(L)** Raw264.7 cells containing vector, Flag-Rubicon WT,  $\Delta$ CCD or  $\Delta$ SR were stimulated with 100 $\mu$ g/ml Texas-Red labeled opsonized-zymosan particles for indicated times, followed by confocal microscopy with  $\alpha$ p22phox and  $\alpha$ Flag. Bar, 2  $\mu$ m. The bottom panel shows the colocalization index (%) between p22phox and zymosan-coated beads (left) or between Rubicon and zymosan-coated beads at 30 min.

**(M, N, and O)** Rubicon expression enhances the co-localization between lysosomes and phagosomes upon zymosan stimulation. Raw264.7 cells containing vector, Flag-Rubicon WT,  $\Delta$ CCD or  $\Delta$ SR were stimulated with zymosan (100 $\mu$ g/ml) for 30min and staining with lysosome dye LysoTracker (50 nM) **(M)** or infected with HK-GFP-*L. monocytogenes* (MOI=1) and a self-

quenched red BODIPY dye-conjugated bovine albumin serum (DQ-Red BSA) (10 $\mu$ g/ml) (**N**), followed by confocal microscopy with  $\alpha$ Rubicon. Bar, 2  $\mu$ m. The right panels show the colocalization index (%) between Rubicon and LysoTracker (**M**) or between Rubicon/Listeria and DQ-Red BSA (**N**), respectively. (**O**) PI(3)KC3 activity upon zymosan treatment. At 24 h posttransfection with p40(phox) PX–EGFP fusion, Raw264.7 cells expressing vector, Rubicon WT, Rubicon  $\Delta$ CCD mutant, and Rubicon  $\Delta$ SR mutant were stimulated with zymosan (100 $\mu$ g/ml) for 30min and subjected to an inverted fluorescence microscope. p40(phox) PX–EGFP-positive vesicles were quantified as the mean  $\pm$  SD of combined results from three independent experiments. Bar, 10  $\mu$ m. WCLs were used for immunoblotting with  $\alpha$ GFP,  $\alpha$ Flag, or  $\alpha$ Actin.

**Figure S4. Rubicon enhances phagocytosis in a p22phox-binding-dependent manner**

(**A**) Raw264.7 cells containing vector, Rubicon WT, or  $\Delta$ SR were infected with HK-GFP-*L. monocytogenes* (MOI=1) for the indicated times, followed by flow cytometry analysis to detect internalized HK-GFP-*L. monocytogenes*. The middle panel shows the treatment with Cytochalasin D (Cyto D, 10  $\mu$ M), phagocytosis inhibitor as a negative control. SC, solvent control. The mean fluorescence intensity values of HK-GFP-*L. monocytogenes* from flow cytometry were used to generate phagocytosis rate kinetics (bottom). (**B**) At 48h postinfection with lentivirus-GFP (MOI=50), lentivirus-shRNA-p22phox (MOI=50) or lentivirus-shRNA-gp91phox (MOI=50), Raw264.7 cells were stimulated with 100 $\mu$ g/ml zymosan-coated particles for indicated times, followed by lysis and sucrose-gradient ultracentrifugation to isolate zymosan bead-containing phagosomal fractions. Phagosomal fractions were subjected to IB with  $\alpha$ gp91phox,  $\alpha$ p22phox,  $\alpha$ p47phox, or  $\alpha$ Rubicon. WCLs were used for IB with  $\alpha$ gp91phox,  $\alpha$ p22phox or  $\alpha$ Actin. (**C**) At 48h postinfection with recombinant Ad-Vector (MOI=200), Ad-Rubicon (MOI=100), or Ad-shRubicon (MOI=200) virus, Raw264.7 cells were stimulated with

100µg/ml IgG-coated particles for indicated times, followed by lysis and sucrose-gradient ultracentrifugation to isolate the bead-containing phagosomal fractions (please see the Method section). Phagosomal fractions were subjected to IB with  $\alpha$ Beclin-1,  $\alpha$ UVRAG,  $\alpha$ gp91*phox*,  $\alpha$ p22*phox*,  $\alpha$ p47*phox*,  $\alpha$ VPS34,  $\alpha$ LC3 or  $\alpha$ Rubicon. Whole cell lysates (WCL) were used for IB with  $\alpha$ Rubicon or  $\alpha$ Actin.

**(D and E)** NADPH oxidase activity is necessary for Rubicon-mediated increased of phagocytosis. **(D)** Raw264.7 cells containing vector, Rubicon WT, or  $\Delta$ SR were infected with HK-GFP-*L. monocytogenes* (MOI=1) for the indicated times, followed by flow cytometry analysis to detect internalized HK-GFP-*L. monocytogenes*. The bottom panels show the treatment with 20 µM DPI or 0.5 mM AEBSF NADPH oxidase inhibitor as a negative control. SC, solvent control. **(E)** Rubicon shows no significant effect on the LPS-, hot-alkali-depleted zymosan or MDP-mediated release of ROS. Raw264.7 cells expressing vector or Flag-Rubicon or BMDMs infected with lenti-GFP or lenti-GFP-Rubicon (MOI=100) were analyzed for NOX activity upon stimulation with 100ng/ml LPS, 200µg/ml hot alkali-treated zymosan, 100µg/ml MDP or 100nM PMA. Quantitative data are the mean  $\pm$  SD of values from three experiments.

### **Figure S5. Rubicon enhances TLR signal transduction**

**(A and B)** Rubicon enhances TLR2 signal transduction. **(A)** Raw264.7 cells containing vector or Flag-Rubicon were stimulated with 100µg/ml zymosan for indicated times, followed (left panel) by IP with  $\alpha$ TLR2 and IB with  $\alpha$ gp91*phox*,  $\alpha$ p22*phox*, and  $\alpha$ MyD88 or (right panel) by IP with  $\alpha$ MyD88 and IB with  $\alpha$ Y257-phospho-specific-MyD88 or  $\alpha$ MyD88. WCL was used for IB with  $\alpha$ TLR2,  $\alpha$ Flag or  $\alpha$ actin. **(B)** Raw264.7 cells containing vector or Flag-Rubicon WT were stimulated with 100µg/ml zymosan for 30min, followed by confocal microscopy with  $\alpha$ TLR2 and  $\alpha$ Rubicon. Bar, 5 µm. The left panel, no Texas-Red labeled opsonized-zymosan particles; the

middle panel, Texas-Red labeled opsonized-zymosan particles with solvent control (SC); and the right panel, Texas-Red labeled opsonized-zymosan particles with the Cytochalasin D (Cyto D, 10  $\mu$ M) treatment. The bottom panel shows the colocalization index (%) between zymosan-coated beads and TLR2 (left) or Rubicon (middle) and or between TLR2 and Rubicon (right).

**(C, D, E, F, G, and H)** Rubicon enhances TLR4 signal transduction and plays an important role in the TLR-NADPH oxidase-mediated anti-microbial pathway.

**(C, D, and E)** Rubicon enhances TLR4 signal transduction. **(C)** Raw264.7, THP-1, A549, and HUVEC cells were used for IB with  $\alpha$ gp91 $phox$  (NOX2),  $\alpha$ NOX4, and  $\alpha$ Rubicon or  $\alpha$ Actin. **(D)** A549 cells containing vector or Flag-Rubicon were stimulated with LPS for the indicated times and used for IP with  $\alpha$ Flag and IB with  $\alpha$ p22 $phox$  or  $\alpha$ NOX4. WCLs were used for IB with  $\alpha$ Flag or  $\alpha$ Actin. **(E)** A549 cells containing vector or Flag-Rubicon were stimulated with 100ng/ml LPS or 100ng/ml BLP for the indicated times in the presence or absence of 20  $\mu$ M DPI NADPH oxidase inhibitor, followed by NOX enzymatic assay. Quantitative data are the mean  $\pm$  SD of values from three experiments. **(F, G, and H)** Rubicon plays an important role in the TLR-NADPH oxidase-mediated anti-microbial pathway. Raw264.7 cells containing vector or Rubicon were stimulated with zymosan (100 $\mu$ g/ml), IFN $\gamma$  (10ng/ml), and/or *L. monocytogenes* (MOI=1) and assayed for NADPH oxidase **(F)**, NO synthase activity **(G)** and intracellular bacterial loads **(H)** as described in Figure 4.

**Figure S6. *In vivo* Rubicon expression in infected mice.**

**(A)** Rubicon expression in the spleen and liver of recombinant Ad-infected mice. At days 2, 7 and 12 post-injection with Ad-vector ( $1 \times 10^{13}$  pfu/kg), Ad-shRubicon ( $1 \times 10^{12}$  pfu/kg), or Ad-Rubicon ( $1 \times 10^{13}$  pfu/kg) *i.v* via tail vein, spleens and livers were taken out to show the expressions of Rubicon. IB with  $\alpha$ Rubicon or  $\alpha$ Actin. **(B)** At 48h post-injection with Ad-vector

( $1 \times 10^{13}$  pfu/kg), Ad-shRubicon ( $1 \times 10^{12}$  pfu/kg), or Ad-Rubicon ( $1 \times 10^{13}$  pfu/kg) twice *i.v* via tail vein, mice were infected with *L. monocytogenes* ( $1 \times 10^6$  CFU/mouse). At 5 days *p.i.* livers and spleens were harvested for IB with  $\alpha$ Rubicon. **(C, D and E)** Doxycycline-inducible, macrophage-specific expression of Rubicon in SRA-rtTA-Rubicon mice. After 7 days of doxycycline treatment, mice were infected with *L. monocytogenes* ( $1 \times 10^7$  CFU/mouse). At 4 days *p.i.* spleens were harvested for IB with  $\alpha$ Flag,  $\alpha$ Rubicon or  $\alpha$ actin **(C)**, immune-stained with  $\alpha$ Mac-3,  $\alpha$ Flag or DAPI **(D)**, and for photograph **(E)**. Bar, 20  $\mu$ m.

**Figure S7. Rubicon plays distinctive roles in conventional and TLR signaling-mediated autophagy.** **(A)** At 48h postinfection with recombinant Ad-Vector (MOI=200), Ad-Rubicon (MOI=100), or Ad-shRubicon (MOI=200) virus, Raw246.7 cells were treated with 2 $\mu$ M rapamycin or 100 $\mu$ g/ml zymosan for indicated times and their cell lysates were used for IB with  $\alpha$ LC3,  $\alpha$ p62,  $\alpha$ Rubicon, or  $\alpha$ Actin. **(B)** Raw264.7 cells containing vector or Rubicon were stimulated with mock (-) or rapamycin (Rapa), starvation (Starv) or zymosan (Zymo) along with solvent control (SC), 10 $\mu$ M 3MA or 200nM Bafilomycin (Baf) pretreatment for 2 h, followed by IB with  $\alpha$ LC3,  $\alpha$ p62, or  $\alpha$ Actin.

## Supplemental Experimental Procedures

### Cell culture

Primary bone marrow-derived macrophages (BMDMs) from 6- to 8-week-old female C57BL/6 mice were prepared. All animals were maintained in a pathogen-free environment. Briefly, bone marrow cells from the femur and tibia were cultured for 4 days in 10% L929 culture media (as a source of M-CSF)-containing Dulbecco's modified Eagle's medium (DMEM; Gibco-BRL) containing 4 mM glutamine and 10% FBS. Mouse macrophage cell line RAW264.7 (ATCC TIB-71; American Type Culture Collection) and HEK293T (ATCC-11268) were maintained in DMEM (Gibco-BRL) containing 10% FBS (Gibco-BRL), sodium pyruvate, nonessential amino acids, penicillin G (100 IU/ml), and streptomycin (100 µg/ml). Human monocytic THP-1 (ATCC TIB-202) cells were grown in RPMI 1640/glutamax supplemented with 10% FBS and treated with 20 nM PMA (Sigma-Aldrich) for 24 h to induce their differentiation into macrophage-like cells, followed by washing three times with PBS. Transient transfections were performed with Lipofectamine 2000 (Invitrogen), or calcium phosphate (Clontech), according to the manufacturer's instructions. RAW264.7 and THP-1 stable cell lines were generated using a standard selection protocol with 4 µg/ml of puromycin.

### Reagents

CHX, BSA, IgG, Cytochalasin D, 3-Methyladenine, Bafilomycin A1, and rapamycin were from Sigma; Zymosan and BLP (Pam2CSK4) were purchased from Invivogen; NAC, DPI, AEBSF, DHE and CM-H<sub>2</sub>DCFDA were from Calbiochem; recombinant mIFN-γ were from eBioscience; Texas Red-conjugated zymosan A (*S. cerevisiae*) BioParticles, LysoTracker Red DND-99 and DQ-Red BSA were from Invitrogen.

## **Bacterial strains**

*L. monocytogenes* and *L. monocytogenes* expressing GFP strains were provided by D. Portnoy (University of California-Berkely), and *M. bovis* BCG and *M. bovis* BCG-GFP strains were provided by Yi Luo (University of Iowa). *L. monocytogenes* and *M. bovis* BCG were grown at 37°C in brain-heart-infusion (BHI) broth medium (BD) and Middlebrook 7H9 medium supplemented with Tween 80, glycerol and OADC (Difco Laboratories), respectively. For all assays, mid-log-phase bacteria (absorbance, 0.9) were used. Batch cultures were aliquoted and stored at -80°C. Representative vials of *L. monocytogenes* and *M. bovis* BCG were thawed and enumerated for viable colony-forming unit (CFU) on BHI agar (BD) and Middlebrook 7H10 agar (Difco), respectively. The effective concentration of LPS was <50 pg/ml in those experiments with a bacterium-to-cell ratio of 10:1. Heat-killed *L. monocytogenes* were obtained by heating for 30 min at 60°C.

## **Autoradiography**

Raw264.7 were labeled for 6h with S<sup>35</sup> Met/Cys (10 µCi/ml; MP Biomedicals, Inc.) in Met/Cys-free DMEM containing dialyzed 10% FBS (Sigma) and 1% L-glutamine (Gibco-BRL), then were stimulated for indicated times at 37 °C with Zymosan or rapamycin and rinsed. 1µg of Flag antibody was added to 1ml of cell lysates and incubated at 4°C for 18h for immunoprecipitation. After addition of protein A/G agarose beads, incubation was continued for 2h. Immunoprecipitates were extensively washed with lysis buffer and eluted with SDS loading buffer by standing on RT for 30 min. After fixing and amplifying, gels were dried and radiolabeled gels were visualized by autoradiography for 18 h.



## **Plasmid construction**

All constructs for transient and stable expression in mammalian cells were derived from the pEBG-GST mammalian fusion vector and the pEF-IRES-Puro expression vector. DNA fragments corresponding to the coding sequences of the human Rubicon, p22*phox*, gp91*phox*, and p47*phox* genes were amplified by polymerase chain reaction (PCR) and subcloned into pEF-IRES-puro between the *Afl*III and *Xba*I sites and selected for stable transfectants. AU1-tagged Rubicon and V5-tagged Beclin1 were cloned into the *Afl*III and *Xba*I sites in pEF-IRES-Puro. GST-tagged Rubicon, p22*phox*, and mutant genes were cloned into a pEBG derivative encoding an N-terminal GST epitope tag between the *Bam*HI and *Not*I sites. Flag-tagged truncated mutant constructs of Rubicon were created by subcloning the PCR products of cDNA fragments containing each domain of the target genes into pEF-IRES-Puro. All constructs were sequenced using an ABI PRISM 377 automatic DNA sequencer to verify 100% correspondence with the original sequence.

## **Yeast two-hybrid screen**

Yeast transformation with human leukocyte cDNA library was performed as recommended by the manufacturers. Briefly, Yeast strain Y187 bearing Gal4-Rubicon full length or C-terminal region fusion gene plasmid was grown overnight in synthetic dropout (SD)/-Trp medium to a density of approximately  $10^7$  cells/ml, then diluted in 1 liter of warmed YPD to an optical density ( $OD_{600}$ ) of 0.2 - 0.3 and grown to exponential stage. Cells were harvested and washed with 100 ml of water twice and TE buffer (Clontech) once. The pellets were resuspended in 8 ml of 10 mM Tris-HCl (pH 7.5), 1 mM EDTA, 0.1 M Li-acetate (LiOAc) and the suspension was mixed with 1 mg of transforming DNA and 20 mg of single-stranded salmon sperm DNA, after which 60 ml of a solution of 40% polyethyleneglycol-4000 in Tris-EDTA-LiOAc was added and mixed thoroughly, followed by incubation at 30°C with agitation for 30 min. After a heat pulse at 42°C for 15 min, cells were pelleted, washed with 50 ml of Tris-EDTA, and plated on selective

medium. Library screening and recovery of plasmids were performed according to manufacturer's instructions (Clontech).

### **Confocal fluorescence microscopy**

For immunostaining, RAW 264.7 and BMDMs cells were seeded on 12-well culture dishes that contained 18 mm diameter round glass coverslips ( $10^5$  cells per well). Cells were fixed with 4% paraformaldehyde in PBS at 4°C for 10 min and permeabilized with 0.25% Triton X-100 in PBS for 15 min before being treated with 10% BSA, 3% FBS for 1 hr at 25°C. Fixed cells were then stained with primary antibodies, including goat anti-p22*phox* (C-17; Santa Cruz Biotech), mouse anti-gp91*phox* (54.1; Santa Cruz Biotechnology), rabbit anti-Flag (Sigma), and rabbit anti-Beclin1 (Cell Signaling) overnight at 4°C. After extensively washing to remove excess primary antibodies with PBS+0.5% Tween20, fixed cells were incubated for 1h at RT with fluorescently labeled secondary antibodies [anti-rabbit IgG-FITC or TRITC, anti-mouse IgG-FITC or TRITC, and anti-goat IgG-Cy5 (Molecular Probes)], followed by extensively washing with PBS+0.5% Tween20 twice and PBS once (each time for 25 min). Cells were imaged with a laser-scanning confocal microscopy (Nikon Eclipse C1)

### **Preparation of Latex Beads**

Polystyrene beads (1.7  $\mu$ m diameter, 2.5% suspension; Polysciences, Inc.) were coated with BSA (100  $\mu$ g/ml), IgG (100  $\mu$ g/ml), Zymosan (1 mg/ml) or PBS (control) for 1h at 37 °C. Beads were washed extensively in PBS before use.

### **Flow cytometry**

Cells were analyzed by flow cytometry for the expression of p22*phox* and gp91*phox* using a FACSCanto II flow cytometer as indicated by the manufacturer (Becton Dickinson). After two washes with PBS, cells were fixed in 2% paraformaldehyde for 10 min at 37°C or permeabilized

by adding ice-cold 100% methanol for 30 min on ice. Cells were stained with primary mAb against p22phox-alexa fluor 488 (CS9, AbD Serotech) or gp91phox alexa fluor 488 (NL7, AbD Serotech) for 30 min at 4°C (1:200). After two washes with PBS, cells were fixed in 4% paraformaldehyde and immediately analysed. In each case, 10,000 cells were acquired. The data were analyzed using BD FACSCanto II (Becton Dickinson).

### **Immunoblotting and immunoprecipitation for membrane bound proteins**

Cells were mechanically scraped in PBS, washed, and then resuspended in Tris buffer (20 mM Tris, 250 mM Sucrose, 2 mM EDTA, 10 mM EGTA, pH 7.5). Cell suspensions were then incubated for 15 min on ice during homogenization with syringe, and centrifuged at 4°C 100,000g for 1 h, to pellet membranes. Supernatants with cytosolic proteins were collected and stored at -20°C until used for immunoblotting or immunoprecipitation. Membrane pellets were repeatedly lysed with Tris-SDS buffer (25 mM Tris, 150 mM NaCl, 1% SDS, 1 mM EDTA, 1 mM EGTA, pH 7.5), and membrane extracts were then prepared by centrifugation at 20°C, 100,000g for 15 min and stored at -80°C until used for immunoblotting or immunoprecipitation. Combined cytosolic and membrane fractions were finally analyzed by immunoblotting or immunoprecipitation with the appropriate corresponding antibodies.

### **Immunoblot analysis and immunoprecipitation**

For immunoblotting, polypeptides were resolved by SDS-polyacrylamide gel electrophoresis (PAGE) and transferred to a PVDF membrane (Bio-Rad). Immunodetection was achieved with V5 (Invitrogen), AU1 (Covance), LC3 (LC3.No.6, Cosmo Bio Co), 4G10 (Upstate), VPS34 (Abgent), and Rubicon (Bethyl Laboratories). Antibodies to Flag and UVRAG from Sigma, GST (Z-5), actin (C4), p22phox (FL-195, 44.1, and C-17), gp91phox (54.1 and H-60), p47phox (H-195), p62/SQSTM1 (D-3), IκBα (C-21), MyD88 (E-11), VPS15 (JK-13) and TLR2 (TL2.1) were purchased from Santa Cruz Biotechnology, Inc. Specific Abs to phospho-(Thr202/Tyr204)-

ERK1/2, phospho-(Thr180/Tyr182)-p38, phospho-(Thr183/Tyr185)-SAPK/ JNK, phospho-IkB $\alpha$ , and Beclin1 were purchased from Cell Signaling Technology. Proteins were visualized by a chemiluminescence reagent (Pierce) and detected by a Fuji Phosphor Imager.

For GST Pulldown, cells were harvested and then lysed in NP-40 buffer supplemented with a complete protease inhibitor cocktail (Roche). Post-centrifuged supernatants were pre-cleared with protein A/G beads at 4°C for 2 h. Pre-cleared lysates were mixed with 50% slurry of glutathione-conjugated Sepharose beads (Amersham Biosciences), and the binding reaction was incubated for 4 h at 4°C. Precipitates were washed extensively with lysis buffer. Proteins bound to glutathione beads were eluted with SDS loading buffer by boiling for 5 min.

For immunoprecipitation, cells were harvested and then lysed in NP-40 buffer supplemented with a complete protease inhibitor cocktail (Roche). After pre-clearing with protein A/G agarose beads for 1 h at 4°C, whole-cell lysates were used for immunoprecipitation with the indicated antibodies. Generally, 1-4  $\mu$ g of commercial antibody was added to 1 ml of cell lysates and incubated at 4°C for 8 to 12 h. After the addition of protein A/G agarose beads for 1 h, immunoprecipitates were extensively washed with lysis buffer and eluted with SDS loading buffer by boiling for 5 min.

### **Protein Purification and Mass Spectrometry**

To identify Rubicon-binding proteins, THP1 cells expressing Flag-Rubicon were stimulated with or without zymosan for 30 min, harvested and lysed with NP-40 buffer (50 mM HEPES, pH 7.4, 150 mM NaCl, 1 mM EDTA, 1% (v/v) NP40) supplemented with a complete protease inhibitor cocktail (Roche). Post-centrifuged supernatants were pre-cleared with protein A/G beads at 4°C for 2 h. Pre-cleared lysates were mixed with  $\alpha$ Flag antibody-conjugated with agarose beads for 4 h at 4°C. Precipitates were washed extensively with lysis buffer. Proteins bound to beads were eluted and separated on a Nupage 4-12% Bis-Tris gradient gel (Invitrogen). After silver staining

(Invitrogen), specific protein bands were excised and analyzed by ion-trap mass spectrometry at the Harvard Taplin Biological Mass Spectrometry facility, and amino acid sequences were determined by tandem mass spectrometry and database searches.

### **Autophagy analysis**

For starvation, cells were washed three times with PBS and incubated in Hank's solution (Invitrogen) for 4 h at 37°C. Cells were treated with Hank's solution or complete medium containing 2 μM rapamycin (Sigma) for 4 h. For the LC3 mobility shift assay or p62 immunoblot, cells were treated for 30 min on ice, lysed with 1% Triton X-100, and then subjected to immunoblotting analysis with an antibody against LC3 or p62.

### **Enzyme-linked immunosorbent assay**

Murine BMDMs, RAW264.7 cells, and THP-1 cells were treated as indicated and processed for analysis by sandwich ELISA. Cell culture supernatants and mice sera were analyzed for cytokine content using BD OptEIA ELISA set (BD Pharmingen) for the detection of TNF-α and IL-6. All assays were performed as recommended by the manufacturers.

### **Production of lentiviral shRubicon or Rubicon**

For silencing of human Rubicon, Oligonucleotide sequences for shRNA interference with Rubicon expression are bp 513-536 of 5' -GAUCGAUGCGUCCAUGUUU- 3', followed by a 9-nucleotide non-complementary spacer (TTCAAGAGA) and the reverse complement of the initial 19-nucleotide sequence. These dsDNA oligonucleotides were cloned into the pGIPZ lentiviral vector (Open Biosystems). Lentiviruses were produced by transient transfection using packaging plasmids (psPAX2 and pMD2.VSV-G purchased from Addgene) after Lipofectamine 2000 mediated transient transfection into 293T cells. Control vector was constructed by

inserting sequences with limited homology to the Rubicon sequences. DNA fragments corresponding to the coding sequences of the Rubicon genes were amplified by PCR and subcloned into pCDH-CMV vector (System Biosciences).

### **Transduction of lentivirus-shRubicon or lentivirus-Rubicon**

Viral-containing media were collected at 72 hr posttransfection and harvested for the viral particles by passing the supernatants through a 0.45  $\mu\text{m}$  filter. The supernatants were used to infect  $2 \times 10^5$  cells in six-well plates in presence of 8  $\mu\text{g/ml}$  Polybrene (Sigma). For lentivirus infection, cells ( $5 \times 10^5$  cells/ml) in DMEM + 10% FBS were seeded in 24-well plates. After 24h, cells were infected with recombinant lentiviruses at various MOIs in the presence of 8  $\mu\text{g/ml}$  Polybrene. On the following day, medium was freshly replaced, and cells were incubated for additional 4 days for Rubicon expression. A parallel experiment using a GFP encoding lentivirus indicated that a minimum of 80% of Raw264.7 and BMDMs cells were transduced by lentiviruses. Titration of lentiviral vectors was determined using 293T cells. Briefly, approximately  $2 \times 10^5$  cells were plated in each well of a six-well plate. On the following day, cells were infected with viral supernatants in the presence of 8  $\mu\text{g/ml}$  Polybrene. After 24h, medium was removed and replaced with fresh medium containing 5  $\mu\text{g/ml}$  puromycin. On day 14, cells were stained with crystal violet for 15 min and colonies were counted using a cutoff of 50 viable cells.

### **Construction of adenoviral shRubicon or Rubicon**

An adenoviruses expressing short hairpin RNA (shRNA) to the Rubicon gene was constructed using the AdEasy system (Stategene). The shRNA oligonucleotides sequences were as follows: 5'-gatcc cc gat aga cag tat atc aga a ttc aag aga t tct gat ata ctg tct atc ttttt a -3', 5'- g gg cta tct gtc ata tag tct t aag ttc tct a aga cta tat gac aga tag aaaaa ttcga-3'. These dsDNA oligonucleotides were cloned into the pSuper vector (OligoEngine) between the *BglIII* and *HindIII*

restriction sites containing the human H1 promoter. The double-strand shRNA oligonucleotides containing the termination signal were inserted at the 3' end of the human H1 promoter and subcloned into the pShuttle vector (Stategene) *NotI* and *HindIII* restriction sites. Control vector was constructed by inserting a sequence that expresses an shRNA with limited homology to the Rubicon sequences. DNA fragments corresponding to the coding sequences of the Rubicon genes were amplified by PCR and subcloned into the pShuttle-CMV vector (Stategene) between the *NotI* and *EcoRV* restriction sites

### **Adenovirus production**

Recombinant adenoviruses were constructed using AdEasy system (Stategene): digested adenovirus vectors with the *Pac I* were transfected into the AD-293 producer cells in a 6-well-plate and cultured with fresh media until cytopathic effect (CPE) was observed. When 80% CPE were observed, recombinant adenoviruses were harvested by repeatedly freezing at  $-80\text{ }^{\circ}\text{C}$  and thawing at  $37\text{ }^{\circ}\text{C}$  four times. Cell lysates were then centrifuged at 2,000g for 30 min at  $25\text{ }^{\circ}\text{C}$  and the supernatants containing recombinant adenovirus particles were stored at  $-80\text{ }^{\circ}\text{C}$ .

All adenoviruses were propagated in AD-293 cells, purified and concentrated by BD Adeno-X™ purification kit (BD Biosciences Clontech). The typical titers were in the range of  $10^{12}$ – $10^{13}$  plaque-forming units (pfu)/mL as determined via plaque assay using 1.25 % SeaPlaque GTG agarose (BioWhittaker Molecular Applications) overlay. A sterile carrier solution [phosphate-buffered saline (PBS)] was used for control injections and dilution of the viruses.

### **Statistical analysis**

All data were analyzed using Student's *t* test with a Bonferroni adjustment or ANOVA for multiple comparisons and are presented as the mean  $\pm$  SD. Differences were considered significant at  $p < 0.05$ . Where indicated, Prism software (Graph Pad) was used for two-way

analysis of variance and Kaplan-Meier survival analyses.